Article

Single Molecule Spectroscopy as a Probe for Dye–Polymer Interactions

Renaud A. L. Valle, Philippe Marsal, Els Braeken, Satoshi Habuchi, Frans C. De Schryver, Mark Van der Auweraer, David Beljonne, and Johan Hofkens

J. Am. Chem. Soc., **2005**, 127 (34), 12011-12020• DOI: 10.1021/ja051016y • Publication Date (Web): 06 August 2005

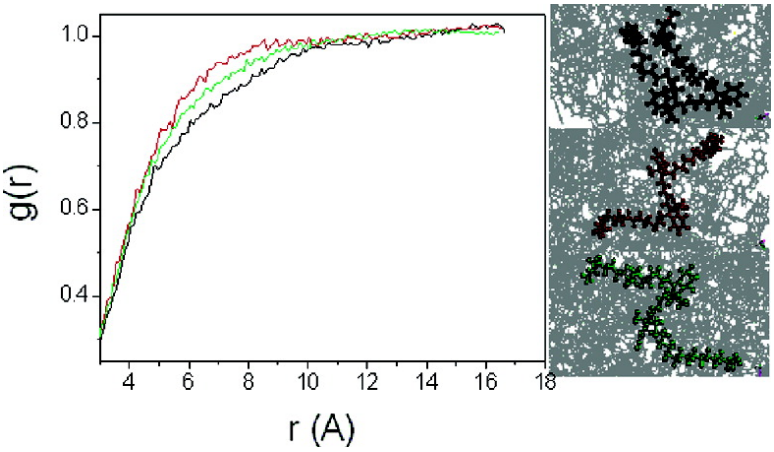

More About This Article

Additional resources and features associated with this article are available within the HTML version:

- Supporting Information
- Links to the 5 articles that cite this article, as of the time of this article download
- Access to high resolution figures
- Links to articles and content related to this article
- Copyright permission to reproduce figures and/or text from this article

View the Full Text HTML

J|A|C|S
ARTICLES
Published on Web 08/06/2005

Single Molecule Spectroscopy as a Probe for Dye−Polymer Interactions

Renaud A. L. Vallée,*,† Philippe Marsal,‡ Els Braeken,† Satoshi Habuchi,† Frans C. De Schryver,† Mark Van der Auweraer,† David Beljonne,‡ and Johan Hofkens*,†

Contribution from the Department of Chemistry, Katholieke Universiteit Leuven, Celestijnenlaan 200 F, B-3001 Leuven, Belgium, and Laboratory for Chemistry of Novel Materials, University of Mons-Hainaut, Place du Parc 20, B-7000 Mons, Belgium

Received February 17, 2005; E-mail: renaud.vallee@chem.kuleuven.be; johan.hofkens@chem.kuleuven.be

Abstract: Experimental (Single Molecule Spectroscopy) and theoretical (quantum-chemical calculations and Monte Carlo and molecular dynamics simulations) techniques are combined to investigate the behavior and dynamics of a polymer−dye molecule system. It is shown that the dye molecule of interest (1,1′-dioctadecyl-3,3,3′,3′-tetramethylindo-dicarbocyanine) adopts two classes of conformations, namely planar and nonplanar ones, when embedded in a poly(styrene) matrix. From an in-depth analysis of the fluorescence lifetime trajectories, the planar conformers can be further classified according to the way their alkyl side chains interact with the surrounding poly(styrene) chains.

I. Introduction

Polymer films with thicknesses of hundreds of nanometers are studied extensively nowadays. The reason for this is twofold. First, they provide ideal sample geometry to investigate the effects of one-dimensional confinement on the structure, morphology, and dynamics of the polymer chains.[1] Second, they are used extensively in technological applications such as optical coatings, protective coatings, adhesives, and packaging materials.

The study of single fluorophores embedded in polymer films has received increasing attention during the past decade. Initially, the polymer matrix was used to immobilize the fluorophores in single molecule studies.[2−5] More recently, an increasing number of investigations have dealt with the reversed situation where the physical properties of polymers are now the focus of these studies using single molecule detection methods.[6−9] At cryogenic temperatures, it has been shown[6] that most of the "spectral trails" of single molecules show a behavior consistent with the double well potential model of glasses, representing motion of a small group of atoms within double well features of the potential energy hypersurface. At higher temperatures, polymer mobility has been probed in the supercooled liquid regime by use of mobility (such as rotational and translational diffusion) observables[7] and in the glassy state by use of spectroscopic observables.[9−13] Very recently, single molecule spectroscopy has allowed us to assess the distribution of local free volume in glassy polymers, using either single dye molecules sensitive to local density fluctuations[9] or dye molecules subjected to conformational changes.[12]

In this paper, we show that an in-depth analysis of single molecule spectroscopy data combined to the input from quantum-chemical calculations and Monte Carlo and molecular dynamics simulations offers a new way to obtain deep insight into the polymer dynamics and polymer−dye molecule interactions at a molecular level.

We present the results of single molecule optical measurements on 1,1′-dioctadecyl-3,3,3′,3′-tetramethylindo-dicarbocyanine (DiD) molecules embedded in a poly(styrene) (PS) matrix. Bimodal spatial distributions of fluorescence lifetimes and spectral widths are observed that are assigned, on the basis of quantum-chemical calculations, to two classes of conformers of the DiD molecule, namely "planar" and "nonplanar" conformers. By comparing the measured temporal lifetime distributions to the lifetime distributions built from Monte Carlo simulations of the system, two "planar" conformers are shown to coexist in the polymer matrix. On the basis of molecular

† Katholieke Universiteit Leuven.
‡ University of Mons-Hainaut.

(1) Roth, C. B.; Dutcher, J. R. Mobility on Different Length Scales in Thin Polymer Films. In *Soft Materials: Stucture and Dynamics*; Dutcher, J. R., Marangoni, A. G., Eds.; Marcel Dekker: 2004.
(2) Macklin, J. J.; Trautman, J. K.; Harris, T. D.; Brus, L. E. *Science* **1996**, *272*, 255.
(3) Xie, X. S.; Trautman, J. K. *Annu. Rev. Phys. Chem.* **1998**, *49*, 441.
(4) Vanden Bout, D. A.; Yip, W.-T.; Hu, D. H.; Swager, T. M.; Barbara, P. F. *Science* **1997**, *277*, 1074.
(5) Veerman, J. A.; Garcia Parajo, M. F.; Kuipers, L.; van Hulst, N. F. *Phys. Rev. Lett.* **1999**, *83*, 2155.
(6) Boiron, A.-M.; Tamarat, Ph.; Lounis, B.; Orrit, M. *Chem. Phys.* **1999**, *247*, 119.
(7) Deschesnes, L. A.; Vanden Bout, D. A. *Science* **2001**, *292*, 255.
(8) Bowden, N. B.; Willets, K. A.; Moerner, W. E.; Waymouth, R. M. *Macromolecules* **2002**, *35*, 8122.
(9) Vallée, R. A. L.; Tomczak, N.; Kuipers, L.; Vancso, G. J.; van Hulst, N. F. *Phys. Rev. Lett.* **2003**, *91*, 038301.
(10) Bartko, A. P.; Dickson, R. M. *J. Phys. Chem. B* **1999**, *103*, 3053.
(11) Vallée, R. A. L.; Cotlet, M.; Hofkens, J.; De Schryver, F. C.; Müllen, K. *Macromolecules* **2003**, *36*, 7752.
(12) Vallée, R. A. L.; Cotlet, M.; Van der Auweraer, M.; Hofkens, J.; Müllen, K.; De Schryver, F. C. *J. Am. Chem. Soc.* **2004**, *126*, 2296.
(13) Tomczak, N.; Vallée, R. A. L.; van Dijk, E. M. H. P.; Kuipers, L.; van Hulst, N. F.; Vancso, G. J. *J. Am. Chem. Soc.* **2004**, *126*, 4748.

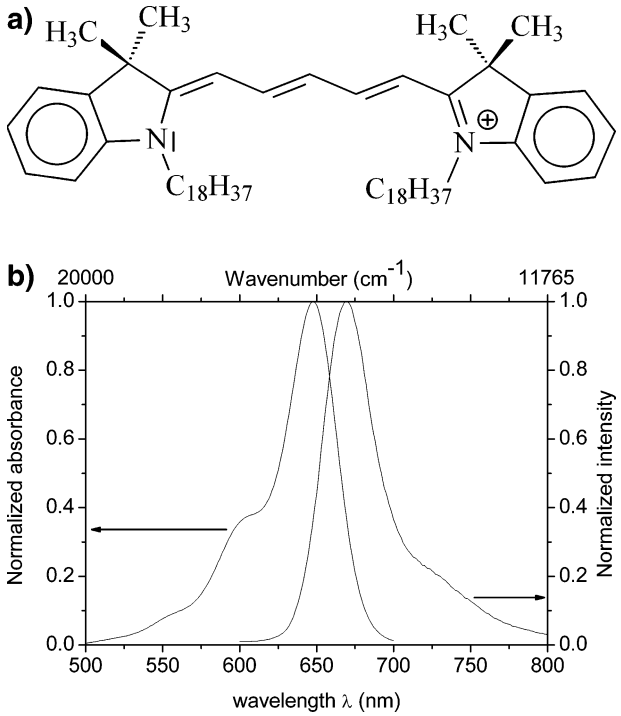

Figure 1. (a) Schematic structure and (b) Absorption and emission spectra of the DiD dye molecule, as measured in a chloroform solution.

dynamics simulations of the dye molecule−polymer system, these two conformers are assigned to molecular structures differing by the relative orientation of their long alkyl chains (positioned either on the same side or on opposite sides with respect to the conjugated backbone of the molecule). This leads to different fractions of holes surrounding the dye molecule and hence different lifetime distributions.

II. Materials and Methods

The polymer films were obtained by spin coating a solution of a nanomolar concentration of the DiD dye in PS (Polymer Standard Service, $M_w = 133\,000$, PI = 1.06, $T_g = 373$ K) on a glass substrate. The dye molecules were excited by pulses of 90 ps at a wavelength λ of 644 nm (Figure 1: the maximum absorbance of the dye molecule is located at $\lambda = 648$ nm, and its maximum emission intensity is located at $\lambda = 670$ nm) and a repetition rate of 10 MHz (PicoQuant) in an inverted confocal microscope (Olympus IX70). The excitation power P was set to 1 μW at the entrance port of the microscope. The emission signal was split equally in two parts. The fluorescence lifetime was measured by use of an avalanche photodiode (SPCM-AQ-15, EG & G Electro Optics) equipped with a time correlated single photon counting card (Becker & Hickl GmbH, SPC 630) used in FIFO mode. Two procedures based on the weighted least-squares (LS) and the maximum likelihood estimation (MLE) method to confidently analyze single-molecule (SM) fluorescence decays with a total number (N) of 500−30 000 counts were used.[14] First, decay profiles were built for each molecule with an integration time of 1s. In this case, the number of counts (5000−30 000) was high enough to fit adequately the profiles with the LS method. The values obtained in this way were used to build the spatial lifetime distribution for all molecules measured in the matrix. Second, to observe the dynamics (lifetime transients) of the single molecules in the polymer matrix, shorter bin sizes have to be taken (100 ms). The decay profiles built on such a time scale count much less photons (500−3000). The MLE method was chosen in this case to fit the decay profiles, as it is known to give stable results over the whole intensity range, even at counts N less than 1000, where the LS analysis delivers unreasonable values. The emission spectra were recorded, with an integration time of 10 s, through a charge coupled device (CCD) camera (Princeton Instruments) fitted with a polychromator (Acton Spectra Pro 150). The experimental spectra are cut by the dichroic mirror (DC-O-660) and the long pass filter (LP660) on the blue edge (25% of the emitted signal transmitted at 655 nm). To determine their width, the spectra were smoothed, by convoluting them with a Gaussian distribution of a 3 nm bandwidth,[15] numerically integrated (in order to determine their area) and divided by the maximum intensity at the peak wavelength. This way of determining the width was chosen as it is the most natural way of defining an effective width of a spectrum, irrespective of its fine structure.

The quantum-chemical calculations were performed using the following methodology. Ground-state optimizations were performed at the semiempirical Hartree−Fock Austin Model 1 (AM1) level[16] and excited-state optimizations by coupling the AM1 Hamiltonian to a full configuration interaction (CI) scheme within a limited active space, as implemented in the AMPAC package.[17] The optical absorption and emission spectra were then computed by means of the semiempirical Hartree−Fock intermediate neglect of differential overlap (INDO) method, as parametrized by Zerner et al.,[18] combined to a single configuration interaction (SCI) technique; the CI active space is built here by promoting one electron from one of the highest sixty occupied to one of the lowest sixty unoccupied levels. To obtain the vibronic progression of the spectra, normal-mode-projected displacements and associated reorganization energies were calculated by the method implemented by Reimers,[19] which is suitable for large molecules. These were then used to simulate the spectra within the framework of a displaced harmonic oscillator model. To take into account the influence of low-frequency external modes, the calculated lines were convoluted with Gaussian lines of 500 cm^{-1} bandwidth, to match the line width of the bulk emission spectrum.

The radiative lifetime has been calculated with the usual formula

$$\tau_0 = \frac{m_e \epsilon_0 c_0^3}{2e^2 \pi \nu_0 f} \quad (1)$$

by further taking into account the renormalization of the photon in the medium: $\epsilon_0 \rightarrow \epsilon_r \epsilon_0$ and $c_0 \rightarrow c_0/n$ and the slight change in the transition frequency.

In this formula, e is the charge of the electron, ϵ_0 and c_0 are the permittivity and the speed of light in a vacuum, and ν_0 and f are the transition frequency and the oscillator strength of the probe molecule in a vacuum, respectively. Finally, the polarizabilities were determined by a sum over states (SOS) method encompassing all states involved in the CI space just mentioned.

The Monte Carlo simulations, allowing us to calculate the radiative lifetime of a dye molecule embedded in a disordered medium, were performed using a homemade software.[20] In these simulations, the spectroscopic properties (transition dipole moment, transition energy, polarizability) of DiD determined by quantum-chemical calculations were used. To model the effect of the environment on the probe molecule, the polarizability of a poly(styrene) base unit (hereafter called styrene unit) was also determined.

(14) Maus, M.; Cotlet, M.; Hofkens, J.; Gensch, T.; De Schryver, F. C.; Schaffer, J.; Seidel, C. A. M. *Anal. Chem.* **2001**, *73*, 2078.
(15) Stracke, F.; Blum, C.; Becker, S.; Müllen, K.; Meixner, A. J. *Chem. Phys.* **2004**, *300*, 153.
(16) Dewar, M. J. S.; Zoebisch, E. G.; Healy, E. F.; Stewart, J. J. P. *J. Am. Chem. Soc.* **1985**, *107*, 3902.
(17) AMPAC, Semichem, 7204 Mullen, Shawnee, KS 66216.
(18) Zerner, M. C.; Loew, G. H.; Kichner, R.; Mueller-Westerhoff, U. T. *J. Am. Chem. Soc.* **2000**, *122*, 3015.
(19) Reimers, J. *J. Chem. Phys.* **2001**, *115*, 9103.
(20) Vallée R. A. L.; Van der Auweraer, M.; De Schryver, F. C.; Beljonne, D.; Orrit, M. *ChemPhysChem* **2005**, *6*, 81.

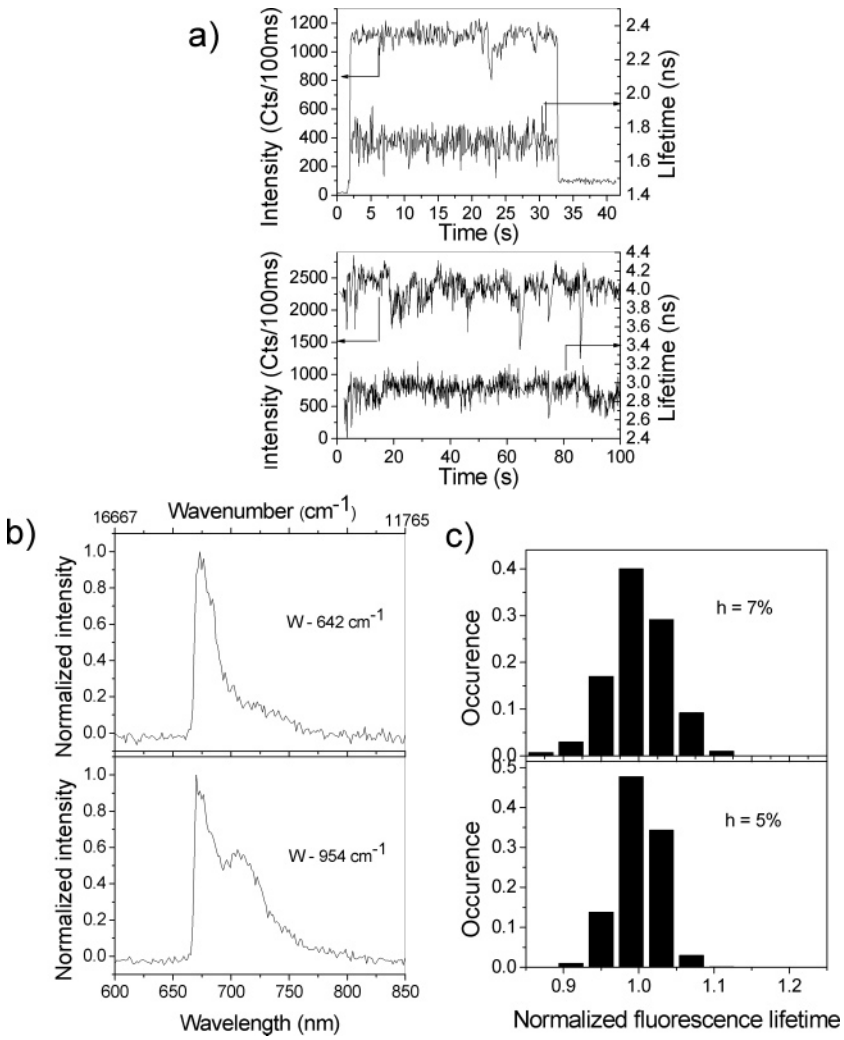

Figure 2. Experimental intensity and fluorescence lifetime time traces (a) and corresponding spectra (b) and distributions (c) of normalized lifetimes, for a planar (top) and a nonplanar (bottom) conformer of the DID molecule embedded in a PS matrix. In (b) the integration time for each spectrum is 10 s. In (c), the lifetime of each conformer is normalized with respect to the mean value of the respective distribution, which is 1.7 ns (2.9 ns) in the case of the planar (nonplanar) conformer.

Molecular dynamics simulations of the DiD molecule−PS system were performed using the Material Studio and Cerius packages by Accelrys. We used the compass[21] force field in order to create an amorphous cell[22] containing a DiD molecule (with its alkyl chains) and two atactic PS chains of 100 monomers each. Ewald summation methods are used to treat Coulombic interactions, and atom based methods are adopted to treat van der Waals interactions with standard cutoffs. All subsequent simulations are performed at a constant number of particles and standard temperature and pressure (NPT ensemble) controlled by a Berendsen thermostat and barostat with a time constant of 145 fs. The Verlet algorithm and a time step of 1 fs are used for all dynamics simulations, which have been run for a total period of 100 ps.

III. Results and Discussion

III.1. Experimental Observations: Existence of Several Species. Cyanine dyes without substituents on the polymethine chain have generally an all-trans geometry in their most stable form.[23] Nevertheless, they exist in several conformers,[24] which can be used to probe particular pockets in microheterogeneous environments. To solubilize the dyes in solvents of low polarity, the nitrogen atoms are substituted by long alkyl chains. Figure 1 shows the structure of DiD (a) and its (room temperature) absorption and emission spectra in a chloroform solution (b). The width of the bulk emission spectrum is $W = 1147$ cm^{-1}.

Figure 2 shows the intensity and fluorescence lifetime time trajectories (a) as well as corresponding spectra (b) of two different representative molecules embedded in a PS matrix. While the first one has a fluorescence lifetime with an average value of 1.7 ns (a, top) and a relatively sharp spectrum (spectral width $W = 642$ cm^{-1}) (b, top) reminiscent of the bulk emission spectrum shown in Figure 1b, the other has a longer average fluorescence lifetime $\tau = 2.9$ ns (a, bottom) and a significantly broader spectrum (spectral width $W = 954$ cm^{-1}) (b, bottom), characterized by an increased amplitude of the 0−1 vibronic peak.

To determine the general character of this behavior and the possible correlation between fluorescence lifetimes and spectra exhibited by the DiD single molecules, an analysis of 164

(21) Sun, H. *J. Phys. Chem. B* **1998**, *102*, 7338.
(22) Theodorou, D. N.; Suter, U. W. *Macromolecules* **1985,** *18*, 1467.
(23) Mishra, A.; Behera, R. K.; Behera, P. K.; Mishra, B. K.; Behera, G. P. *Chem. Rev*. **2000**, *100*, 1973 and references therein.
(24) Vranken, N.; Jordens, S.; De Belder, G.; Lor, M.; Rousseau, E.; Schweitzer, G.; Toppet, S.; Van der Auweraer, M.; De Schryver, F. C. *J. Phys. Chem. A* **2001**, *105*, 10196.

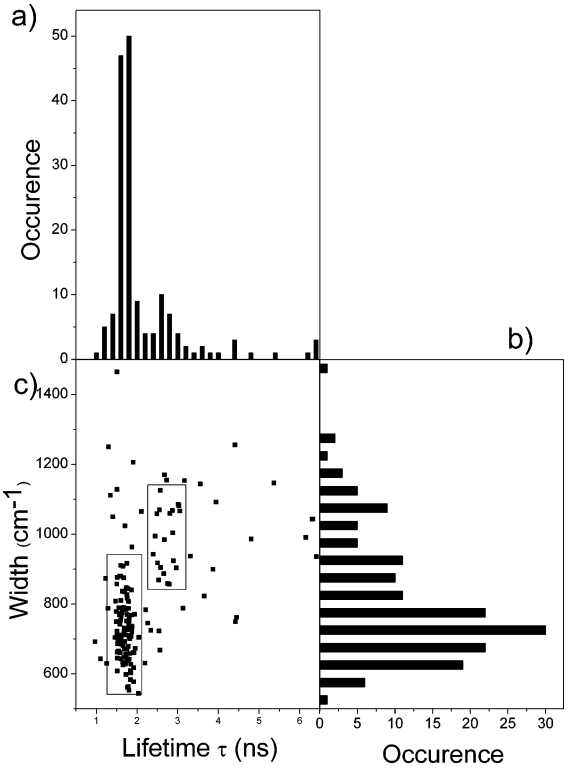

Figure 3. Fluorescence lifetime (a) and spectral width (b) distributions of DiD molecules embedded in a PS matrix. (c) Corresponding correlation plot between fluorescence lifetimes and spectral widths.

molecules embedded in the matrix and surviving irreversible photobleaching for a sufficient period to allow a measurement with good counting statistics (at least 20 000 counts) was performed.

Figure 3 shows histograms of the fluorescence lifetime (a) and spectral width (b) of the single molecules spatially distributed in the polymer matrix. Bimodal distributions of lifetimes and spectral widths are observed. The main and second peaks of the lifetime distribution are located at $\tau \sim 1.8$ ns and $\tau \sim 2.6$ ns, respectively. Similarly, the main and second peaks of the spectral width distribution correspond to a width of $W \sim 700$ cm^{-1} and $W \sim 1100$ cm^{-1}, respectively. The fluorescence lifetimes are shown to be correlated with the spectral widths (Figure 3c), longer fluorescence lifetimes being associated with larger spectral line widths.[25]

III.2. Quantum-Chemical Calculations: Conformational Search. The changes in the spectroscopic observables might be related to the existence of different stereoisomers of the DiD molecule. To check this hypothesis, a search for all possible conformers of DiD was performed at the quantum-chemical level. This was achieved by optimizing the geometries obtained by cis (C)−trans (T) isomerization of each dihedral angle

(25) To draw the boxes shown in Figure 3c, we have proceeded in the following way. We first centred each of them on the lifetime axis exactly at the positions of the first and second peaks in the lifetime distribution (projections from Figure 3a to 3c). The width of the box in lifetime is determined by continuity of the density of points around the center. We proceeded in the same way on the line width axis. For the right upper box, we had to find a compromise between centering the box at the position of the second peak in the line width distribution (projection from Figure 3b to 3c) and the argument of continuity of the density of points within the box. As the two peaks are not so nicely resolved in this case, compared to the lifetime distribution, we decided to favor the continuity argument, which explains why the center of the right upper box is lower than the projection of the second peak in line width.

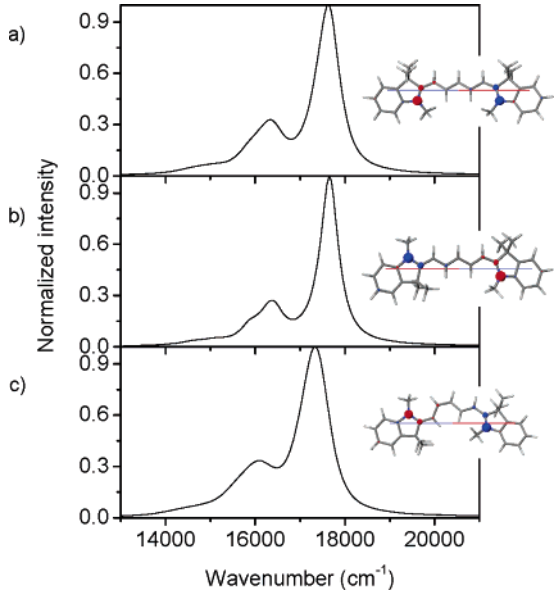

Figure 4. Molecular structure and atomic transition densities associated with the lowest optically allowed electronic excitation of the CTTTTC (a), TTTTTC (b), and CTCTTC (c) conformers. The arrow represents the orientation of the total transition dipole moment. Corresponding calculated emission spectra are also represented.

involved in the polyenic segment joining the nitrogen atoms (Figure 1a). We have used the Hartree−Fock semiempirical Austin Model 1 (AM1) technique to describe both the geometric and electronic structures in the S_0 singlet ground state and S_1 lowest singlet excited state of the studied molecules. Frequency calculations were performed to validate the existence of the local minima uncovered.

Since the DiD molecule has 6 dihedral angles between the N atoms with either cis (C) or trans (T) conformation of the bonds, 2^6 combinations, leading to 64 possible conformers, can be considered. However, some of the 64 conformations can be ruled out right away. This is the case for structures characterized by three consecutive cis conformations along the molecular chain (20 conformers out of the 64), as a result of important sterical constraint. In addition, a number of conformations are identical upon a rotation around the C_2 axis going through carbon 3 of the methine chain (among the 44 conformers left, 19 can be eliminated on the basis of symmetry arguments). 18 of the 25 left conformers lie at an energy much higher (with respect to kT) than that of the global minimum (in the range 2.6−23.5 kcal/mol). This energy difference implies a Boltzmann population below 1% for those molecules, which are therefore very unlikely to be observed. Four of the seven remaining conformers, possessing either zero (1) cis bond or two cis separated by four trans bonds, display almost planar geometries (these are hereafter referred to as TTTTTT, TTTTTC, CTTTTC, TTCTTT). The three others, with several cis bonds close to the center of the polyenic segment, correspond to nonplanar conformers. In all cases, the atomic transition densities are mainly localized on the nitrogen atoms. Figure 4 shows the geometric structures of the three most stable conformers (two "planar" and one "nonplanar") among the seven. Table 1 collects the excited-state properties of the seven conformers, as determined by INDO/SCI calculations on the basis of the AM1 excited-state geometries.

Table 1. Relative Heats of Formation (AM1 ground-state geometries); Transition Energies *E*, Oscillator Strengths *f*, Lengths *l* (distance between the N atoms) of the Transition Dipole Moments and Average Electron−Hole Distances *d* (at the INDO/SCI level on the basis of AM1 excited-state geometries) for the seven most stable stereoisomers of the DiD molecule[a]

conformer	relative heat of formation (kcal/mol)	*E* (eV)	*f*	*l* (10^{-10} m)	*d* (10^{-10} m)
TTTTTT	259.61	2.18	1.80	9.77	6.90
TTTTTC	258.97	2.19	1.74	9.26	7.00
CTTTTC	258.38	2.19	1.68	8.31	7.08
TTTCTC	260.03	2.16	1.50	9.17	6.58
TTCTTT	261.00	2.15	1.48	8.87	6.65
CTCTTC	259.49	2.16	1.36	8.10	6.69
CTTCTT	260.54	2.16	1.34	7.42	6.76

[a] T (C) denotes a trans (cis) linkage along the polyenic segment (see text).

Table 2. Fluorescence Lifetimes τ_f (at the INDO/SCI Level), Polarizabilities χ (INDO/SCI/SOS), Spectral Widths *W*, and Boltzmann Occurrences p_B taking into account degeneracy for the seven most stable stereoisomers of the DiD molecule

conformer	τ_f (ns)	χ (10^{-30} m^3)	W (cm^{-1})	p_B
TTTTTT	1.70	55.7	1048	0.05
TTTTTC	1.75	54.5	1055	0.31
CTTTTC	1.81	53.6	1291	0.43
TTTCTC	2.08	51.2	1156	0.05
TTCTTT	2.13	51.3	1107	0.01
CTCTTC	2.30	49.3	1477	0.13
CTTCTT	2.33	49.1	1430	0.02

A careful analysis of this table reveals that (i) the transition energies of the planar geometries are slightly larger (by about 0.03 eV) than those of the nonplanar geometries. This is a surprising result as the planar conformers should be characterized by a more extended delocalization. Table 1 shows that the transition energies obtained at the INDO/SCI level are correlated with the average electron−hole (e−h) distances, which are larger in the extended planar structures. So, the small variation of the INDO/SCI excitation energy across Table 1 results from partial cancellation between the red-shift induced by increased delocalization and the blue-shift resulting from larger e−h separation upon switching from a nonplanar to a planar conformation. (ii) The oscillator strengths calculated for the seven conformers increase simply as a function of the distance *l* separating the N atoms. As a consequence of (i) and (ii), the radiative lifetime of the dye molecule is a monotonic decreasing function of the distance separating the two N atoms (Table 2).

III.3. Experiment versus Theory. The radiative lifetimes calculated for the seven most stable DiD conformers as a function of their relative occurrence (based on Boltzmann statistics) are displayed in Figure 5a.

By comparing with experimental data (Figure 3), one can readily assign the main measured peak centered on $\tau = 1.8$ ns to the planar conformers, while the presence of other conformers (and especially the CTCTTC stereoisomer, Figure 4) accounts for the second peak in the bimodal lifetime distribution. Note the excellent agreement between the measured and calculated lifetimes. Figure 4 also shows the emission spectrum simulated for each of the three most stable conformers and Table 2 collects relevant data concerning the fluorescence lifetime, spectral line width, and Boltzmann occurrence of the seven conformers.

The calculated emission spectra of the abundant planar TTTTTC (Figure 4b) and nonplanar CTCTTC (Figure 4c) conformers fit reasonably well the measured spectra (Figures 2b top and bottom respectively). The difference in the spectral line widths between both conformers is due to coupling between electronic excitations and low-frequency vibrational modes in the nonplanar structure (resulting from a change in conformation toward a more planar structure when going from the ground state to the excited state). Figure 5c shows the correlation plot between calculated fluorescence lifetimes and spectral widths for the seven conformers. The boxes drawn encompass the most abundant species and clearly correlate with their experimental counterparts (Figure 3c).

III.4. Influence of Local-Field Effects. Up to now, we have paid attention to spatial distributions of fluorescence lifetimes and spectra of DiD molecules in the PS matrix. Single molecule spectroscopy allows one to probe not only spatial but also temporal distributions of spectroscopic observables. Figure 2c,

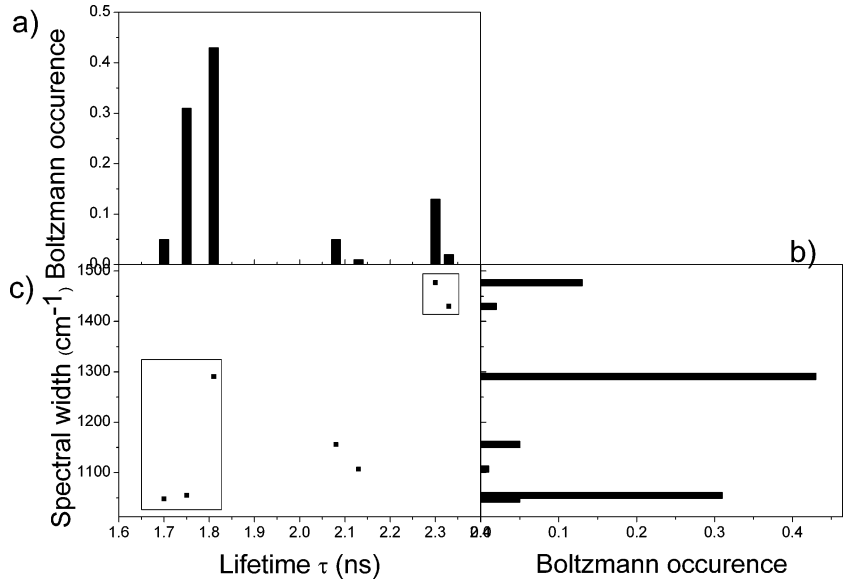

Figure 5. Calculated fluorescence lifetime (a) and spectral width (b) distributions of DiD molecules embedded in a PS matrix. (c) Corresponding correlation plot between fluorescence lifetimes and spectral widths. Note the resemblance with Figure 3.

for example, shows the temporal distributions of normalized fluorescence lifetimes for two different molecular conformations assigned as planar (top) and nonplanar (bottom). Very recently, we have shown, by using either a macroscopic[9,26] or a microscopic[20] approach, that the temporal fluorescence lifetime fluctuations of a DiD molecule are mainly due to local density fluctuations of the surrounding polymer matrix: a given fraction of holes is "moving" around the probe molecule, thereby modifying the local field experienced by the molecule.

On a microscopic scale, a medium consists of discrete atoms or molecules. According to the Lorentz virtual cavity model,[27] a sphere is defined whose radius R is much less than the wavelength of light and greater than the intermolecular distance. The molecules within the sphere are considered as point dipoles, which are embedded in a continuous, isotropic, dielectric medium. To take into account (1) the elongated shape (Figure 4) and specific polarizability of the probe molecule investigated here and (2) the presence of both monomer units and holes around the probe molecule in a polymer matrix (inhomogeneity of the matrix), we have recently extended the Lorentz's model.[20]

The probe molecule is considered as an extended dipole of length l (l being the N−N separation) and polarizability χ (values given in Tables 1 and 2). This view is fully supported by the INDO/SCI calculated atomic transition density distributions that show major contributions on the N atoms (Figure 4). In our simulations, the probe is located at the origin of a 3D cubic lattice and surrounded by z polarizable monomers of polarizability α (calculated to be 1.0×10^{-39} C^2 m^2/J at the INDO/SCI/SOS level). To mimic the motion of the styrene units around the fixed probe molecule, a given fraction of holes (with zero polarizability) is introduced in the lattice. To determine the lattice constant Δ, the van der Waals volume of a styrene unit $V = 119 \times 10^{-30}$ m^3 is simply attributed to the volume $V = \Delta^3$ of a cell in the cubic lattice. After excitation by a laser pulse, the probe molecule, characterized by an emission transition dipole moment μ, spontaneously emits a photon that polarizes the surrounding monomer units. The dipoles μ_k induced on the surrounding monomers, considered as point dipoles, are obtained from the set of coupled equations (k encompasses both probe and solvent molecules):

$$\mu_k = \alpha_k[E(r_k) + \sum_{j=1,j\neq k}^{z} \hat{T}_{kj} u_j] \tag{2}$$

where $E(r_k)$ is the electric field generated by the source dipole at position r_k of the lattice and $\hat{T}_{kj}$ is the dipole−dipole interaction tensor:

$$\hat{T}_{kj} = \frac{1}{r_{kj}^3}\left(\hat{I} - \frac{3 r_{kj} r_{kj}}{r_{kj}^2}\right) \tag{3}$$

where $\hat{I}$ is the identity tensor and $r_{kj} = r_k - r_j$.

The second term in eq 2 includes interactions between the monomers once they have been polarized (polarizabilities $\alpha_k = \alpha$) and "back" interactions between the polarized monomers and the polarizable probe molecule (polarizability $\alpha_k = \chi$). The local electric field felt by the probe molecule is thus the sum of all electric fields experienced by the surrounding monomers and of the reaction field induced by all these polarized monomers that act back on the probe molecule.

At this level, all interactions between molecules inside the Lorentz sphere have been taken into account, and one can define an effective transition dipole moment μ_{tot}, which is the sum of the molecular dipole moment (source dipole) μ and of all induced dipoles μ_k within the discretization sphere:

$$\mu_{tot} = \mu + \mu_k \tag{4}$$

with μ_k given by eq 2.

To take into account the influence of the continuous dielectric medium surrounding the Lorentz sphere on the radiative lifetime, we simply introduce the Lorentz local field factor in the description. The spontaneous emission rate $1/\tau_f$ of the probe molecule embedded in the disordered medium thus finally can be written as

$$\frac{1}{\tau_f} = \left(\frac{\epsilon + 2}{3}\right)^2 \left|\frac{\mu_{tot}}{\mu}\right|^2 \frac{1}{\tau_0} \tag{5}$$

with τ_0 given by eq 1. The near-field effect of the disordered heterogeneous medium on the radiative lifetime can thus be evaluated completely once the ratio $|\mu_{tot}/\mu|^2$ between the total dipole in the cavity and the source dipole associated with the probe molecular charge distribution is known. As described above, this is achieved upon classical electrostatic calculations based on eqs 2−4.

To build a statistical distribution of the fluorescence lifetimes τ_f of a DiD molecule embedded in a PS matrix, Monte Carlo realizations of one representative conformer (either the planar TTTTTC or the nonplanar CTCTTC conformation) of the molecule surrounded by styrene units and holes have been achieved. A Monte Carlo run is implemented in the following way: (1) The fraction of holes (threshold value) is first fixed. (2) For each cell on the lattice, a uniformly distributed (between 0 and 1) random number is chosen. (3) If the random number falls below the threshold value, then the given cell is occupied by a hole, or else the cell is occupied by a monomer. The Monte Carlo simulations are repeated typically 1000 times for each given threshold value.

Figures 6 and 7 show the results of these Monte Carlo simulations in the case of the planar TTTTTC and nonplanar CTCTTC conformers, respectively, for a hole fraction ranging from $h = 1\%$ to $h = 10\%$ by a step of 1%. In both cases, the distributions of the normalized fluorescence lifetimes τ_r reduce to single bars centered on $\tau_r = 1$, for $h = 0\%$ (not shown). For $h = 1\%$, the distributions are very narrow and symmetric around $\tau_r = 1$. For h ranging from 2% to 10%, the distributions are getting broader and more asymmetric. The increased asymmetry, which shows up as an increase of the tail of the distributions on the long lifetime side, is slightly more pronounced in the case of the TTTTTC conformer than for the CTCTTC conformer. A detailed study reveals that the asymmetry toward higher fluorescence lifetimes is a simple consequence of the fact that a hole placed longitudinally with respect to the dipole axis of the molecule causes a large upward departure of the fluorescence lifetime with respect to its average, while a hole placed transversally only causes a small downward shift.[22]

(26) Vallée R. A. L.; Tomczak, N.; Kuipers, L.; Vancso, G. J.; van Hulst, N. F. *J. Chem. Phys.* **2005**, *122*, 114704.
(27) Böttcher, C. J. F. *Theory of electric polarization*, 2nd ed.; Elsevier: Amsterdam, 1973; Vol. 1.

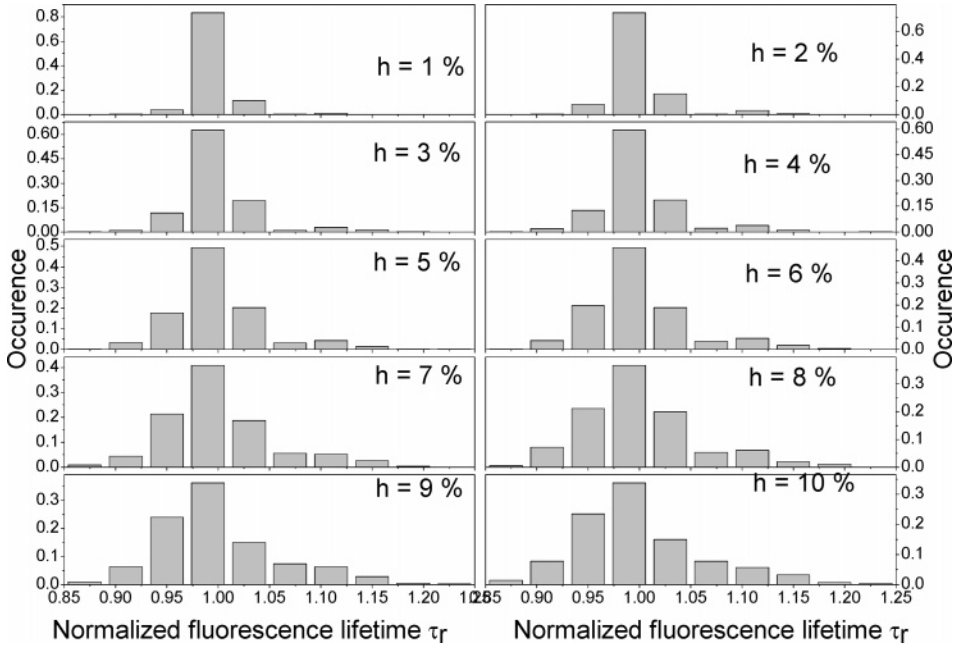

Figure 6. Fluorescence lifetime distributions of the TTTTTC stereoisomer after 1000 Monte Carlo runs. The cubic lattice is filled with six shells of polarizable monomers surrounding the extended dipole of polarizability χ, located at the origin. Holes are placed at random positions on the lattice with a fraction $h =$ 1% to $h = 10\%$ from top left to bottom right.

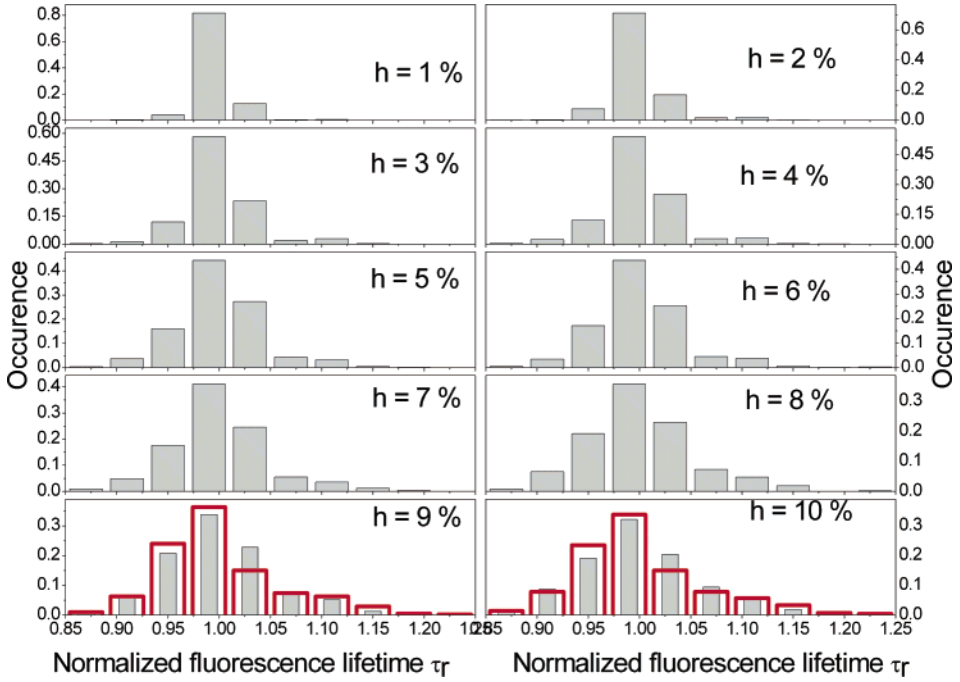

Figure 7. Same as Figure 6 for the CTCTTC conformer. For $h = 9\%$ and 10%, the normalized lifetime distributions (red) of the TTTTTC conformer are superimposed to those of the CTCTTC conformer. These distributions of the TTTTTC conformer are clearly more asymmetric than those of the CTCTTC conformer.

In addition, this effect increases with increasing polarizability of the probe molecule in comparison to that of the medium, which explains the more pronounced asymmetry found for the TTTTTC conformation (as this conformation displays both larger transition dipole moment and polarizability).

III.5. Experimental Validation of Fluctuations in Lifetimes due to Local Field Effects. Figure 2c shows the distributions of normalized fluorescence lifetimes for a planar (top) and a nonplanar (bottom) conformation of the DiD molecule embedded in a PS matrix, as identified from their average lifetimes (obtained from the lifetime trajectories, Figure 2a) and spectral shapes (Figure 2b). The distribution measured for the planar structure (top) is found to be slightly broader than that for the nonplanar structure (bottom). In both cases, the existence of such distribution points to the influence of the nanoenvironment on the probe molecule, which in our picture relates to the fraction of holes h that surrounds the probe molecule. To get a rough estimate of h, the measured lifetime distribution has been superimposed to the distributions predicted from Monte Carlo simulations for a broad range of h values (Figures 6, 7). The

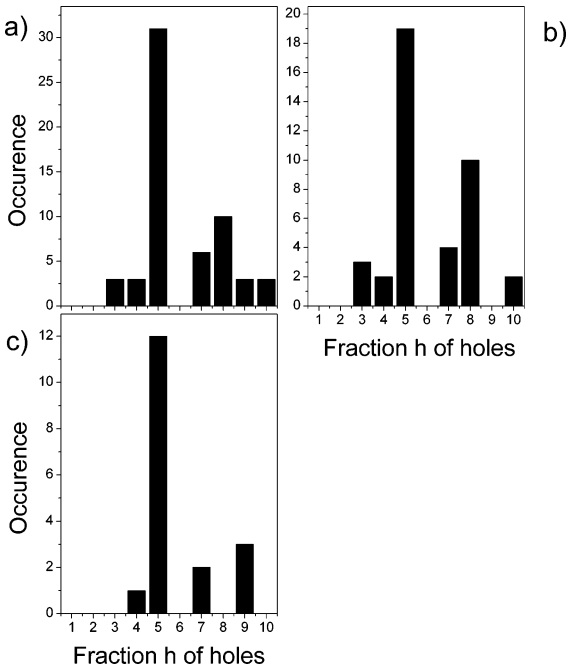

Figure 8. (a) Distribution of the fraction *h* of holes surrounding the DiD molecules embedded in the PS matrix. The distribution of holes surrounding planar and nonplanar conformers is given in (b) and (c), respectively.

best fit between experiment and theory is achieved for $h = 7\%$ in the case of the planar structure and $h = 5\%$ for the nonplanar one (Figure 2c).

The analysis, performed for these two molecules (Figure 2), has been extended to all molecules included in the boxes drawn in Figure 3c that survived a photobleaching event for more than 10 s, allowing us to get at least 100 occurrences of the fluorescence lifetime and to build up reliable histograms. A total number of 57 molecules was analyzed in this way. Among these, 39 molecules can be classified as planar from their emission characteristics. Figure 8 shows the distributions of the fraction of holes *h* surrounding a given molecule by considering (a) both planar and nonplanar conformers, (b) only planar molecules, and (c) only nonplanar molecules. Note that, since we only considered molecules belonging to the boxes drawn in Figure 3 where the fluorescence lifetimes are clearly correlated with the spectral widths, the belonging of a molecule to the planar or nonplanar category is unambiguous.

Very interestingly, the *h* distribution obtained for the planar conformers exhibits a bimodal character[28] (Figure 8b) with peaks at 5% and 8%, while the distribution (Figure 8c) obtained for the nonplanar conformer is monomodal with $h = 5\%$. The bimodal character of the distribution for the planar conformers points to the observation of possibly two conformers of this type, tentatively assigned as the TTTTTC and CTTTTC (Figure 4) conformers, as both are very stable (Tables 1 and 2) according to the quantum-chemical calculations.

III.6. Molecular Dynamics Simulations. The main difference between the two planar conformers lies in the position of the N atoms (to which the long alkyl chains are attached) with respect to the conjugated backbone of the molecule. In the case of the CTTTTC planar conformer, the two N atoms are on the same side, while for the TTTTTC planar conformer, the N atoms are on opposite sides with respect to the conjugated backbone (Figure 4). The nonplanar CTCTTC conformer also has its N atoms on opposite sides with respect to the conjugated backbone. This suggests that the species to be associated with $h = 5\%$ (Figure 8) are the conformers with N atoms on opposite sides and, therefore, the peak at $h = 8\%$ should be assigned to the planar CTTTTC conformer (Figure 4a). Because of the close proximity of the two alkyl chains lying on the same side of the CTTTTC backbone, these chains are expected to interact strongly with each other thereby hindering the segments of the polymer chains to approach the molecule closely and leading to an increased free volume in the close proximity of the dye molecule. On the contrary, for the other two species, the alkyl chains, located on opposite sides with respect to the conjugated skeleton, are free to interact with the polymer chains and should thus be more anchored in the PS matrix.

To check this hypothesis, we have performed molecular dynamics simulations for each conformer of the DiD molecule embedded in a poly(styrene) box comprising two chains of 100 monomers. Figure 9a shows three snapshots of such simulations, corresponding to the CTTTTC (black), TTTTTC (red), and CTCTTC (green) conformers. Figure 9b shows six (two alkyl chains per conformer) time trajectories for the dihedral angle comprising the first four carbon atoms of the alkyl chains attached to the N atom, as provided by these simulations in a 100 ps time scale (the angle is measured by a step of 5 ps). For such a system, the relaxation time related to thermalization, i.e., the time it takes for the non bonded interactions to relax, is about 20 ps (as revealed on a graph plotting the non − bonded interaction versus time, not shown). The vertical bar drawn in Figure 9b marks this limit, over which the fluctuations of the dihedral angles become significant. Figure 9b shows that the dihedral angles are changing considerably in time for the planar CTTTTC conformer (black lines). In contrast, small variations of the dihedral angles are observed in the case of the planar TTTTTC (red lines) and nonplanar CTCTTC (green lines) conformers.

Another very important marker for the amount of local ordering and packing of the system is the pair distribution function $g(r)$, which describes the averaged (over time) density of poly(styrene) at a distance r from the reference molecule. Such pair distribution functions are shown in Figure 9c for the CTTTTC (black line), TTTTTC (red line), and CTCTTC (green line) conformers. At long enough distances (∼12 Å) from the reference molecule, the pair distribution function tends in all cases to the limiting value of the average poly(styrene) density. Interestingly, $g(r)$ displays different evolutions for the different conformers at smaller r values (in the range 4−10 Å), associated to differences in the packing of the poly(styrene) chains: the red curve (planar conformer with the alkyl chains on opposite sides with respect to the conjugated backbone) indeed shows much faster saturation to the limiting value of the polystyrene density than the black curve (planar conformer with the alkyl chains on the same side with respect to the conjugated backbone). The green curve (nonplanar conformer with the alkyl chains on opposite sides with respect to the conjugated backbone) follows closely the red curve.

(28) The depth of the "dip" between both maxima at 5% holes and 8% holes exceeds the standard deviation on the occurrence. The latter equals (assuming a Poisson distribution) the square root of the occurrence. This amounts to 4.4 and 3.2 for 5% and 8% holes, respectively. On the other hand, the probability for the minimum occurrence at 6% holes to be 0 at an expectation value of 3 events or more is less than 0.05. Hence one can safely assume the distribution to be bimodal.

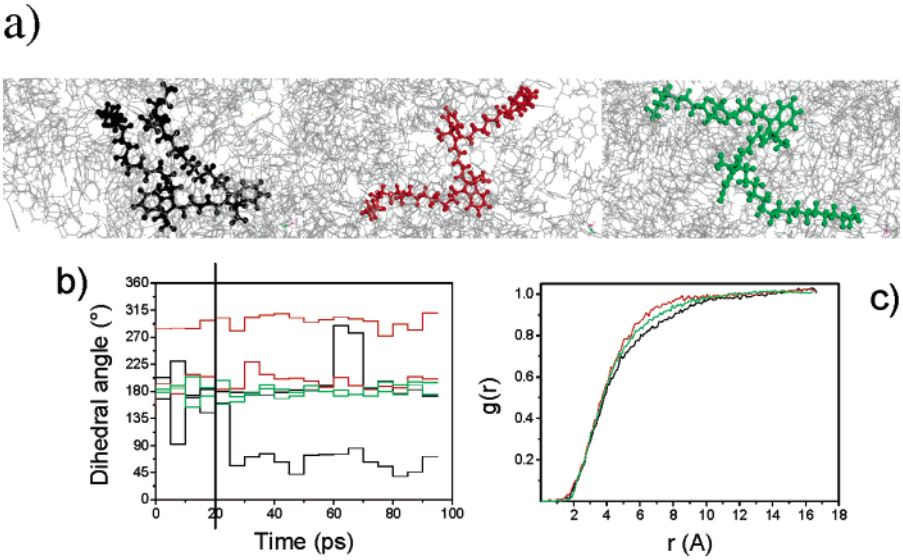

Figure 9. Snapshots (a), time trajectories of the dihedral angles comprising the first four carbon atoms of the long alkyl chains attached on the N atoms (b) and pair distribution functions g(r) (c) obtained from molecular dynamics experiments of the CTTTTC (black), TTTTTC (red) and CTCTTC (green) DiD conformers in a poly(styrene) box consisting of 2 chains with 100 monomers.

These results confirm the following: (i) In the case of the planar molecule with the alkyl chains on the same side of the molecule, the steric interactions between the two chains lead to highly mobile side chains, which hinder the polymer chains from coming close to the molecule and results in an increased local free volume. (ii) In case the alkyl chains are situated on opposite sides of the molecule, their interaction with the polymer chains is favored, which leads to a reduced mobility of the system and thus a lower free volume.

Conclusions

Two subpopulations (bimodal distributions of the fluorescence lifetimes and spectral widths) of the DiD molecule are found (Figure 3) to coexist in a poly(styrene) matrix. The two different species are easily identified from the correlation observed between their fluorescence lifetimes and spectral widths (Figure 3c). As is, the first population is characterized by a fluorescence lifetime around $\tau_f = 1.8$ ns and a spectral width around $W = 700$ cm^{-1}. The second population has a slightly longer lifetime around $\tau_f = 2.6$ ns and a significantly broader spectrum, with a spectral width around $W = 1100$ cm^{-1}. Quantum-chemical calculations have allowed assigning these two subpopulations to two different classes of conformers of the DiD molecule. In brief, within the seven most stable conformers found (Table 1), two of them, the almost all-trans planar molecules (TTTTTC, CTTTTC), are found to have both calculated fluorescence lifetimes (Figure 5a) and spectral widths (Figure 5b, Table 2) compatible with the observed first subpopulation. These are referred to as the planar molecules. The second subpopulation, with a longer lifetime and increased spectral width, is assigned to the other nonplanar molecules (Figure 4), of which the most abundant is the CTCTTC conformer (Table 2, Figure 5).

After having unambiguously established the existence of and assigned the two observed subpopulations of DiD molecules in the PS matrix to planar and nonplanar conformers, the local behavior of the polymer directly surrounding the probe molecule has been investigated. A polymer medium is a highly disordered medium. Chains in the matrix are coiled and entangled so that cooperative motion along the chain is not easy. Only local motions of chain segments are allowed. But these motions require a certain amount of space or holes in the system, which is equivalent to free volume. Free volume is always present due to the poor packing of the chains in the system. As shown recently in the literature, temporal fluctuations of the fluorescence lifetime of a DiD molecule embedded in a poly(styrene) matrix (Figure 2a) can be attributed to the motion of chain segments and thus holes around the probe molecule.[9,20,25] Free volume is modeled hereby putting voids, i.e., sites of zero-polarizability, in the lattice representing the medium (section 3.4). Monte Carlo simulations of the lifetime fluctuations arising from changes in local field factors (as obtained by applying classical electrodynamics theory on the basis of a quantum-chemical input for the characteristics of the probe and the styrene units) have been performed (Figures 6 and 7) for representative conformers and various fractions of holes. Comparing the experimental normalized radiative lifetime distributions (Figure 2a) to the simulated ones then allows an estimate of the fraction of holes surrounding each single DiD molecule. For conformers with the alkyl chains situated on opposite sides (trans-conformers) with respect to the conjugated backbone, a fraction $h = 5\%$ of voids locally surrounding the molecules has been found while this fraction is raised to $h = 8\%$ in the case of the planar conformer with alkyl chains on the same side with respect to the conjugated backbone. Molecular dynamics simulations clearly suggest that the increased fraction of holes surrounding the DiD conformer in the latter case is due to the steric hindrance between the two chains on the nitrogen atoms, which leads to a decreased packing density, an increased local free volume resulting in a higher mobility of the alkyl side chains. On the contrary, for the trans-conformers, the alkyl chains interact more strongly with the surrounding polymer chains, thus lowering mobility and local free volume.

Single molecule spectroscopy proves to be a method of choice to investigate the various conformations of a dye molecule and their interactions with the surrounding polymer matrix.

Acknowledgment. R.A.L.V. thanks the FWO for a postdoctoral fellowship. D.B. is a research associate from FNRS. The

KULeuven Research Fund, the Federal Science Policy through the IAP/V/03, the Flemish Ministry of Education through GOA/1/2001, the European programs LAMINATE and NAIMO, the FNRS (FRFC 9.4532.04), and the FWO are gratefully acknowledged for supporting this research.

JA051016Y